

Supplementary information for the paper

Adventures in co-crystal land: high Z', stoichiometric variations, polymorphism and phase transitions in the co-crystals of four liquid and solid cyclic carboxylic acids with the supramolecular reagent isonicotinamide

Andreas Lemmerer* and Manuel A. Fernandes

Table S1. Hydrogen bonds for **1** [Å and °].

D-H...A	d(D-H)	d(H...A)	d(D...A)	<(DHA)
N(1A)-H(1AS)...O(1B)	0.88	2.07	2.948(3)	175
N(1A)-H(1AA)...O(3A)#1	0.88	2.07	2.926(3)	164
N(1B)-H(1BS)...O(1A)	0.88	2.07	2.947(3)	175
N(1B)-H(1BA)...O(3B)#2	0.88	2.04	2.897(3)	165
N(1C)-H(1CS)...O(1D)	0.88	2.08	2.961(3)	174
N(1C)-H(1CA)...O(3C)#2	0.88	2.06	2.918(2)	166
N(1D)-H(1DS)...O(1C)	0.88	2.06	2.937(3)	177
N(1D)-H(1DA)...O(3D)#1	0.88	2.08	2.941(3)	166
N(1E)-H(5ES)...O(1F)	0.88	2.08	2.958(3)	173
N(1E)-H(5EA)...O(3E)#1	0.88	2.06	2.920(3)	166
N(1F)-H(1FS)...O(1E)	0.88	2.06	2.938(3)	177
N(1F)-H(1FA)...O(3F)#2	0.88	2.12	2.980(3)	166
N(1G)-H(1GS)...O(1H)	0.88	2.07	2.947(2)	177
N(1G)-H(1GA)...O(3G)#1	0.88	2.09	2.951(3)	166
N(1H)-H(1HS)...O(1G)	0.88	2.06	2.924(3)	169
N(1H)-H(1HA)...O(3H)#2	0.88	2.03	2.893(3)	165
N(1I)-H(1IS)...O(1J)	0.88	2.08	2.961(3)	175
N(1I)-H(1IA)...O(3I)#1	0.88	2.13	2.993(2)	166
N(1J)-H(1JS)...O(1I)	0.88	2.07	2.940(3)	172
N(1J)-H(1JA)...O(3J)#2	0.88	2.07	2.933(3)	166
N(1K)-H(1KS)...O(1L)	0.88	2.07	2.948(3)	175
N(1K)-H(1KA)...O(3K)#2	0.88	2.11	2.974(3)	167
N(1L)-H(1LS)...O(1K)	0.88	2.09	2.962(3)	172
N(1L)-H(1LA)...O(3L)#1	0.88	2.05	2.913(3)	165
O(2A)-H(2A)...N(2A)	0.84	1.77	2.605(3)	170
O(2B)-H(2B)...N(2B)	0.84	1.78	2.608(3)	171

O(2C)-H(2C)...N(2C)	0.84	1.80	2.631(3)	171
O(2D)-H(2D)...N(2D)	0.84	1.77	2.603(3)	172
O(2E)-H(2E)...N(2E)	0.84	1.80	2.628(3)	170
O(2F)-H(2F)...N(2F)	0.84	1.77	2.603(3)	171
O(2G)-H(2G)...N(2G)	0.84	1.77	2.607(2)	172
O(2H)-H(2H)...N(2H)	0.84	1.78	2.609(3)	168
O(2I)-H(2I)...N(2I)	0.84	1.77	2.603(3)	171
O(2J)-H(2J)...N(2J)	0.84	1.81	2.637(3)	168
O(2K)-H(2K)...N(2K)	0.84	1.77	2.608(3)	171
O(2L)-H(2L)...N(2L)	0.84	1.78	2.609(2)	169

Symmetry transformations used to generate equivalent atoms:

#1 x+1,y,z #2 x-1,y,z

PXRD confirming bulk quantification.

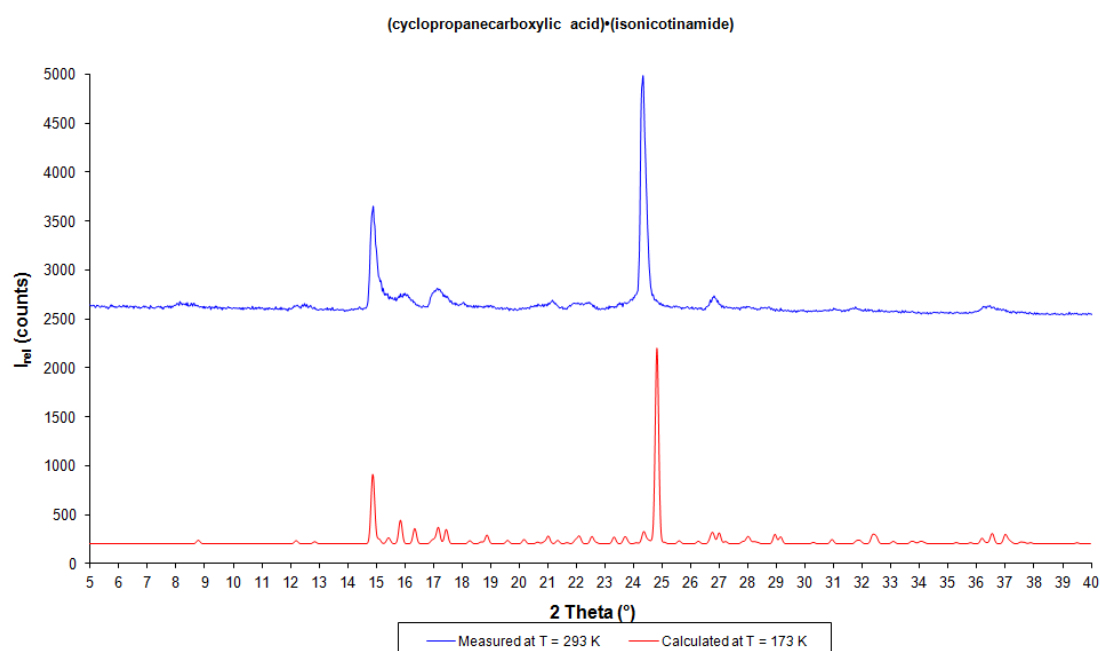


Figure S1. Comparative calculated and measured PXRD pattern for **1**.

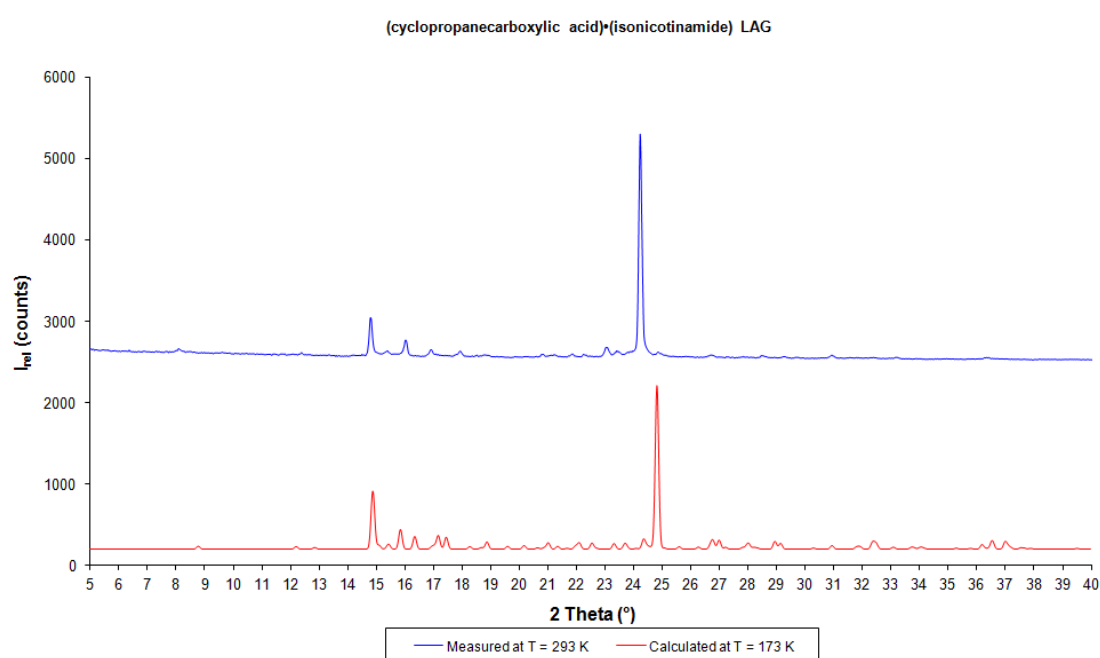


Figure S2. Comparative calculated and measured PXRD pattern for **1** from Liquid-Assisted Grinding.

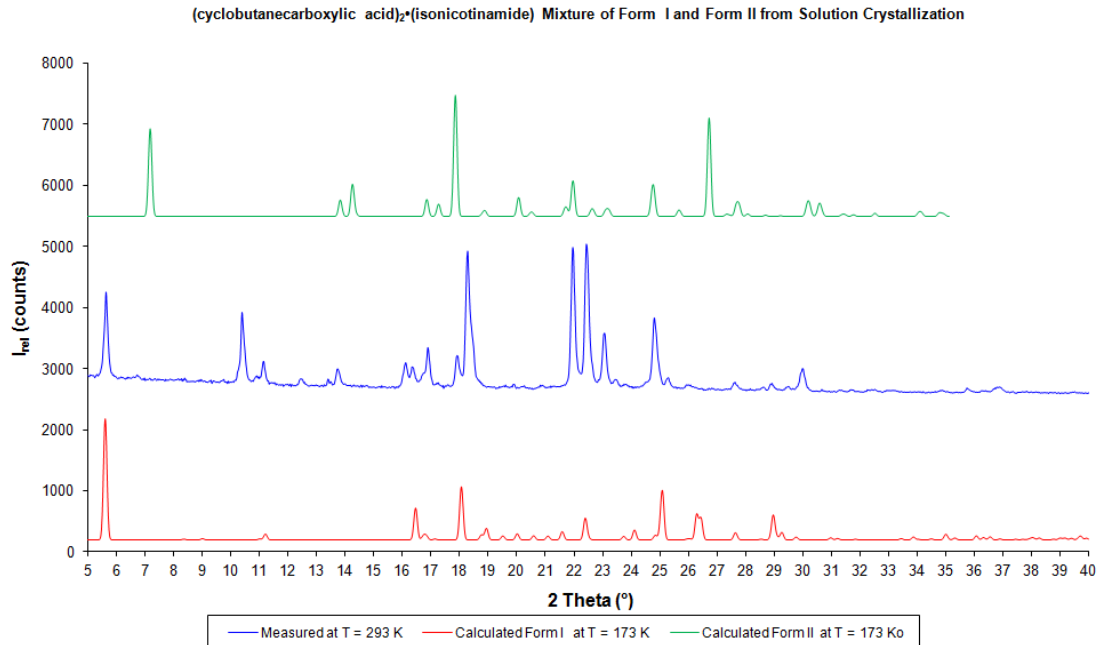


Figure S3. Comparative calculated and measured PXRD pattern for **2a** and **2b**.

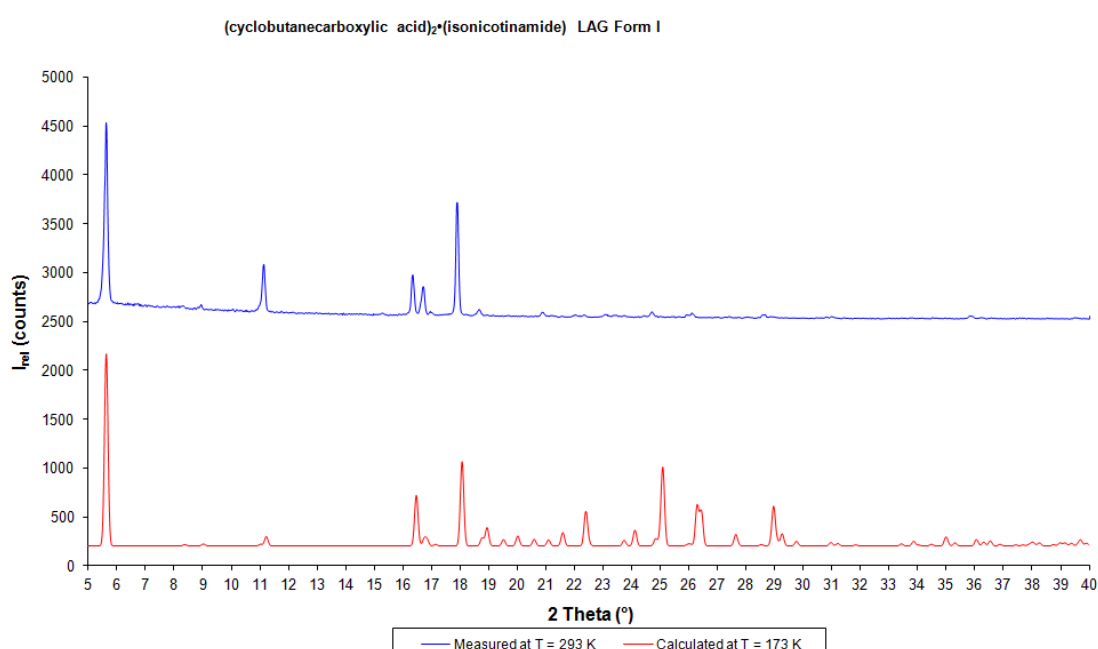


Figure S4. Comparative calculated and measured PXRD pattern for **2a** from Liquid-Assisted Grinding.

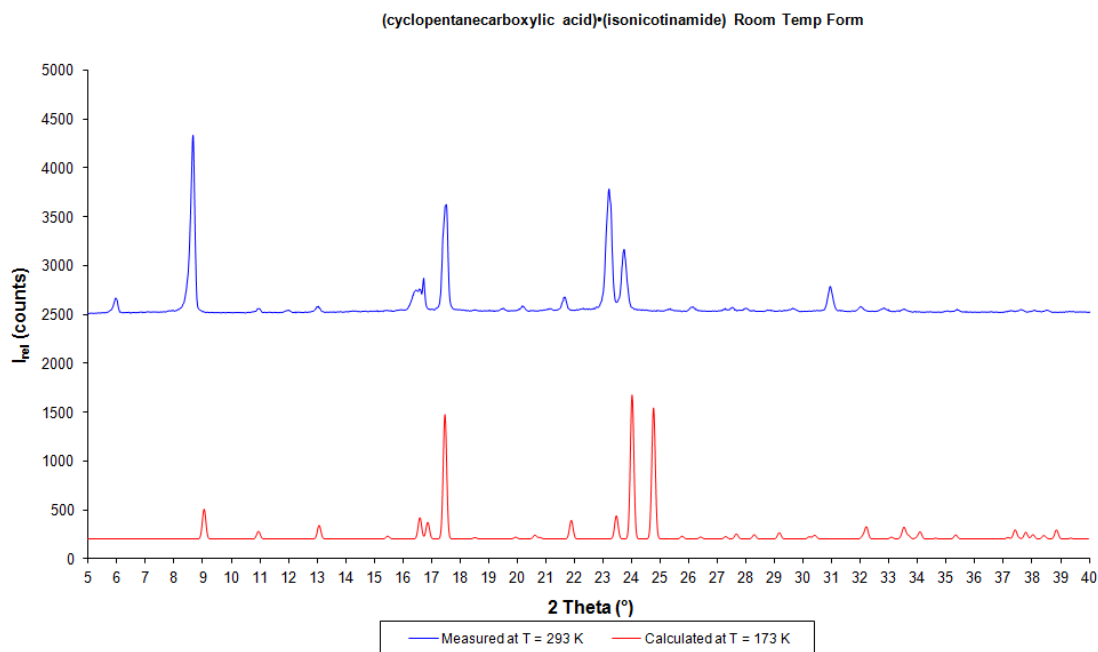


Figure S5. Comparative calculated and measured PXRD pattern for **3**.

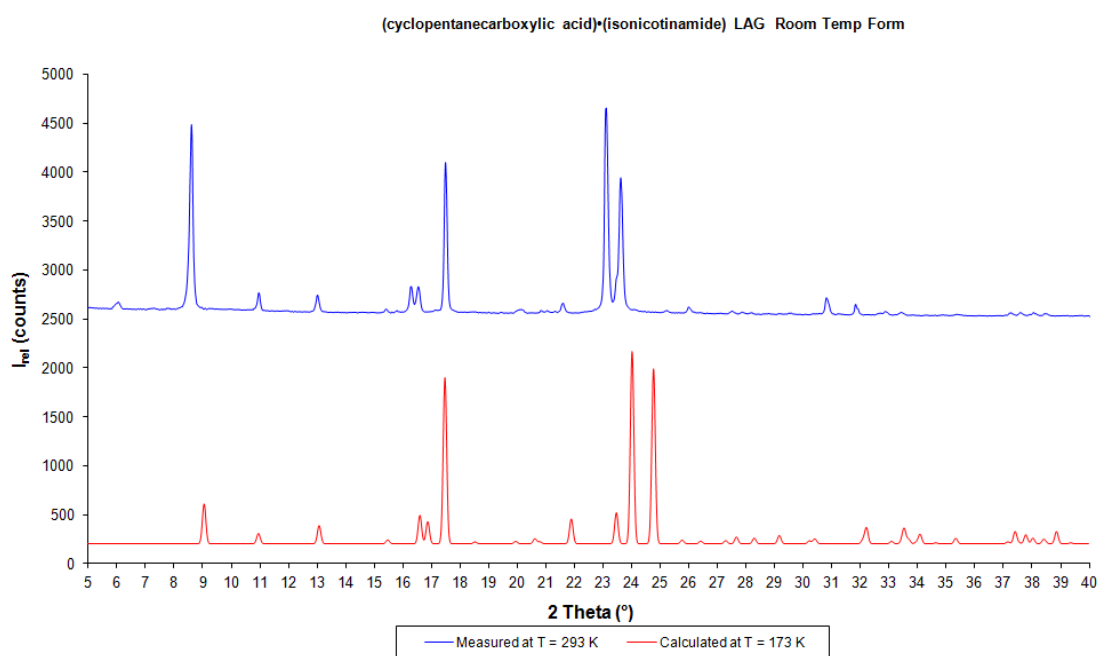


Figure S6. Comparative calculated and measured PXRD pattern for **3** from Liquid-Assisted Grinding.

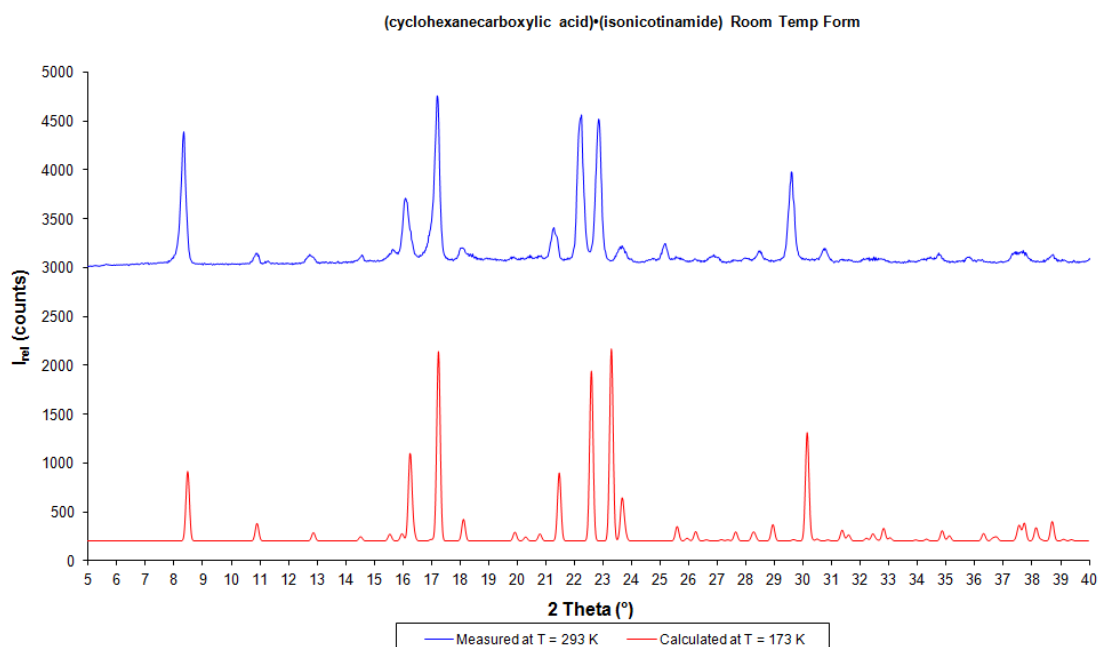


Figure S7. Comparative calculated and measured PXRD pattern for **4a**.

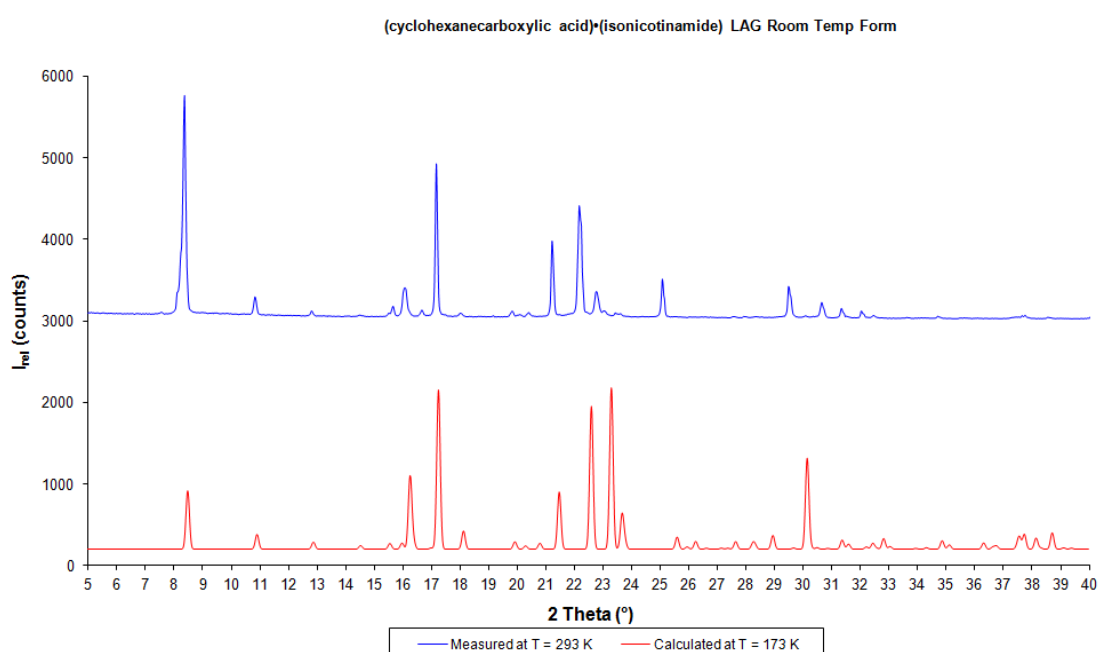


Figure S8. Comparative calculated and measured PXRD pattern for **4a** from Liquid-Assisted Grinding.

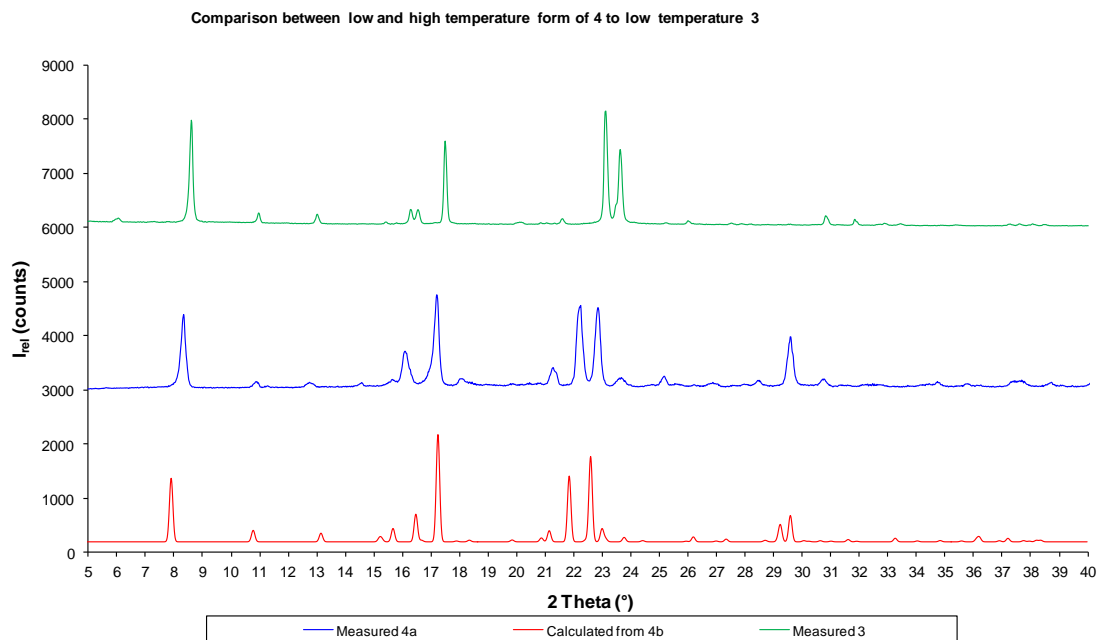


Figure S9. Comparative between the PXRD patterns of the isostructural **3** and **4a** and **4b**.

IR Spectra confirming formation of co-crystals

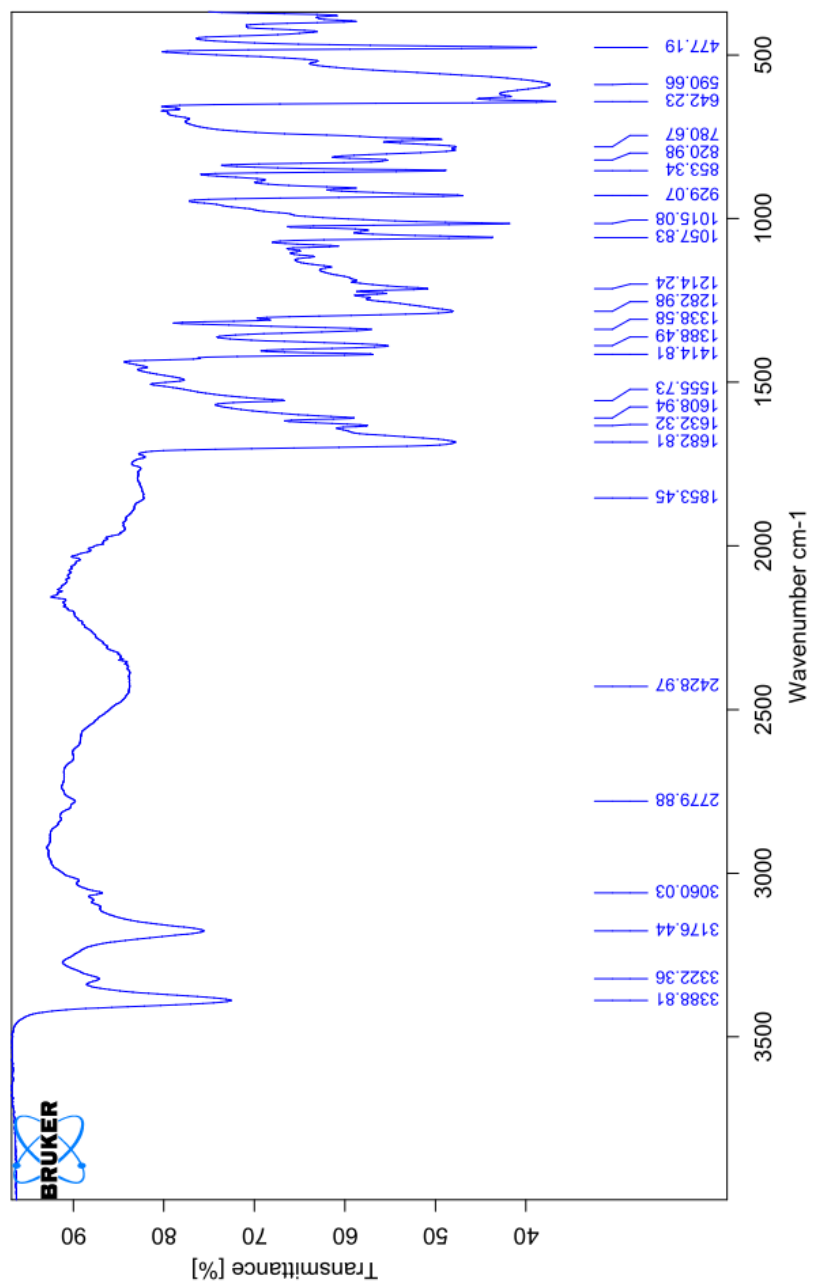


Figure S10. IR trace for **1**.

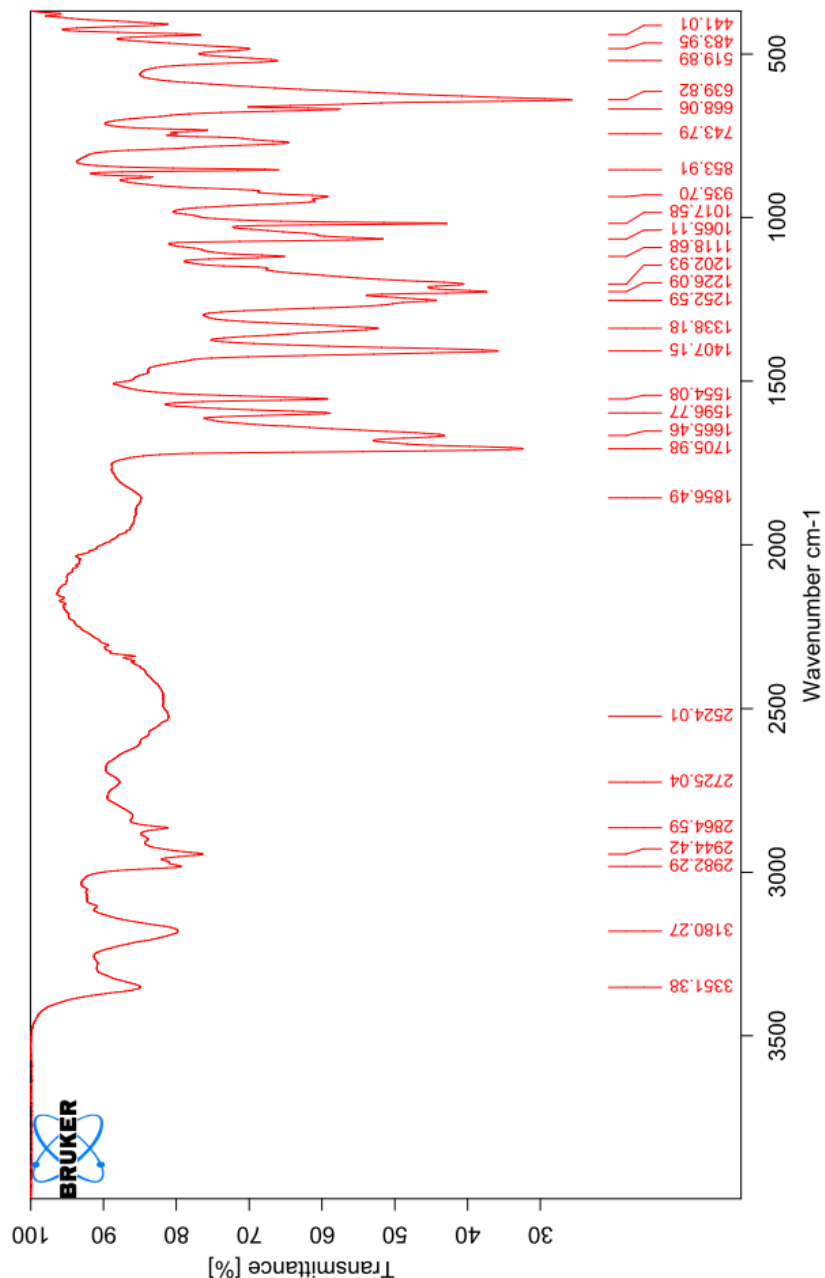


Figure S11. IR trace for 2a.

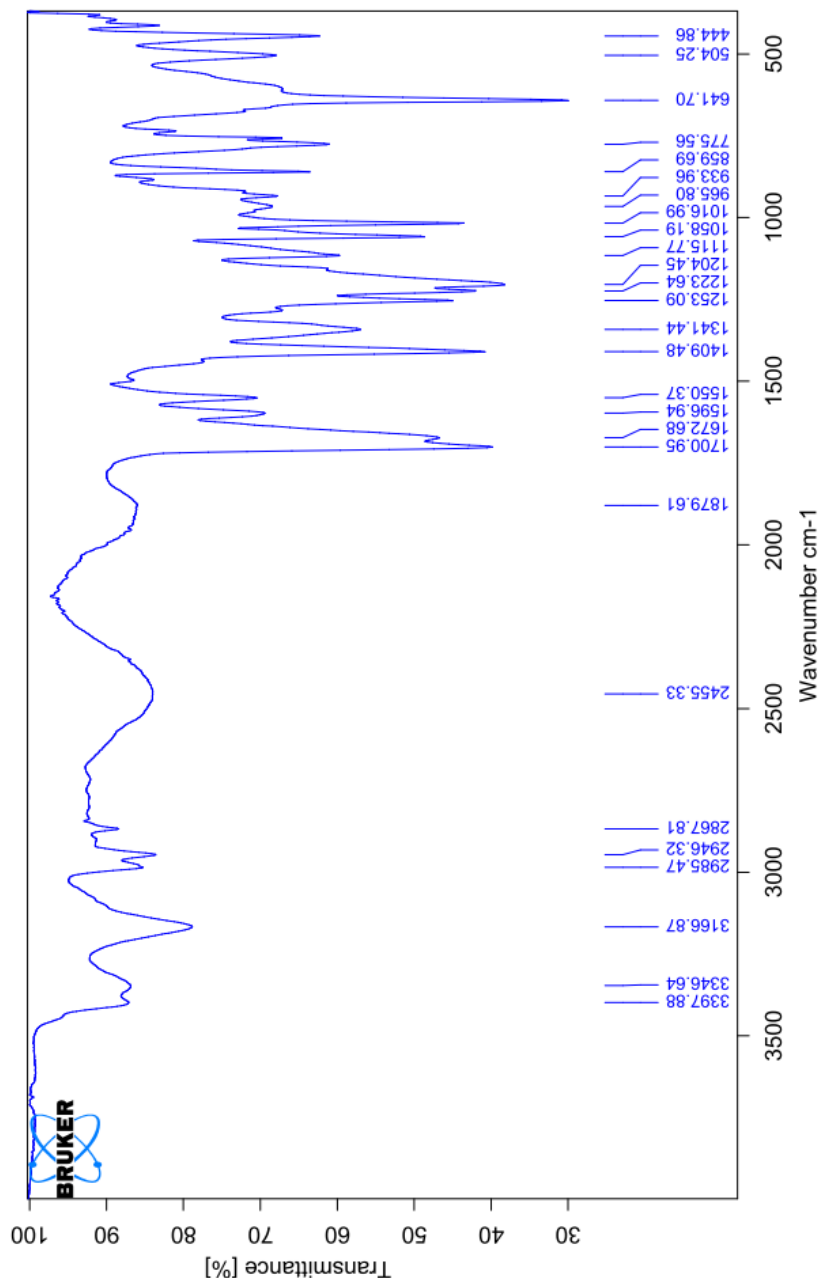


Figure S12. IR trace for 2b.

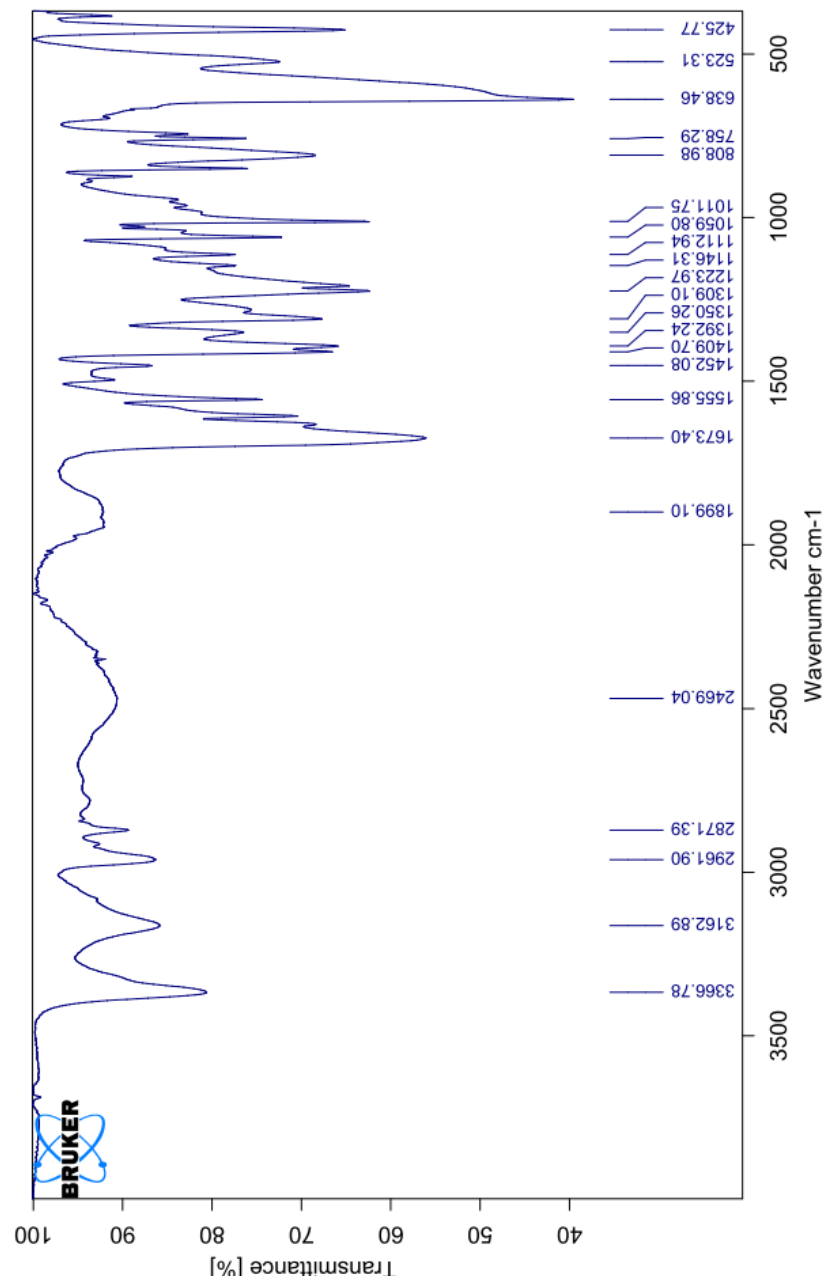


Figure S13. IR trace for 3.

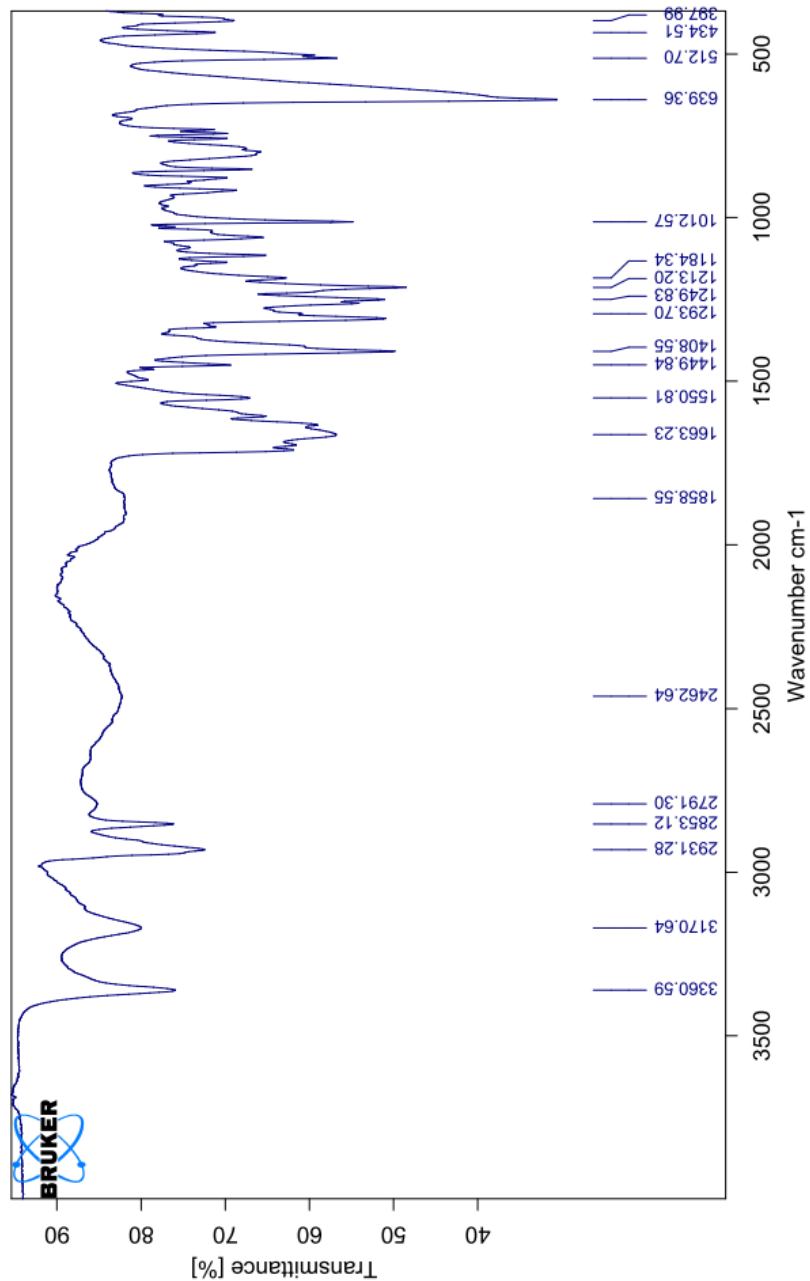


Figure S14. IR trace for 4a.

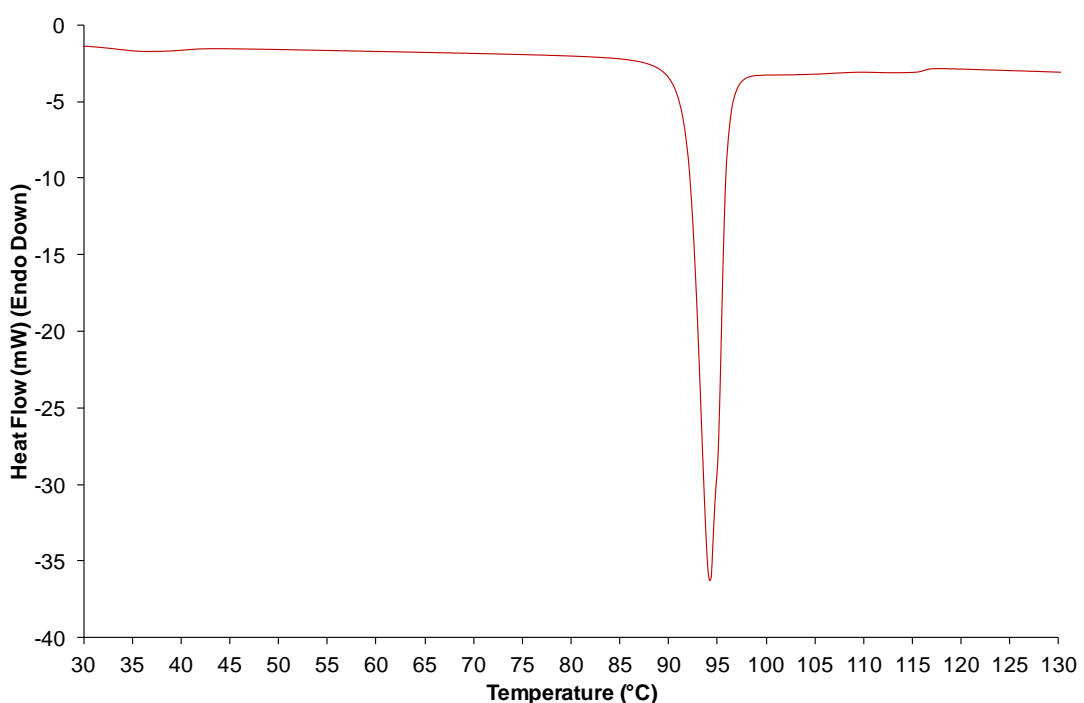


Figure S15. DSC trace for **1**.